

# **Exploring the Pendulum with Constant and Time-Periodic Forcing**

Applied Project MATH 303 — Fall 2021

Mengfan Gong  
Chenyu Wang

October 21, 2021

## Abstract

The dynamic behavior of Josephson junctions driven by DC currents (without AC current) and the pendulum behavior subjected to constant time periodic forces have been previously studied analytically by other scholars. In our paper, we numerically analyze the resistor-capacitor shunt junction model (RCSJ model) of Josephson junctions driven by AC currents and focused on the effect of amplitude variation of external oscillatory force on the dynamical system. The phase portrait, equilibria and stability are discussed. Particularly, the change in the number of equilibria, the stability of the system and the dynamic change process of the solutions are explored by bifurcation diagrams and Poincare mappings.

By observing the bifurcation diagrams under purely alternating currents, we conclude that the solutions of the system are periodic when the amplitude (AC current) is relatively small. As the AC current increases, the system starts entering chaos. Although periodic solutions or even bifurcations may appear after chaos appears for the first time, they would disappear gradually and go back to chaos later, which means chaos is the main circumstance after the system appears the first chaos. What's more, We also analyze the effect of the angular velocity  $\omega$  and the damping factor  $\beta$  in the dynamical system. It is found that as  $\beta$  increases, the moment when the system first goes from a periodic solution to chaos is delayed, i.e. the critical AC current that needs for system to appear first chaos is larger. And as  $\omega$  increases, the moment when the system first appears chaos will be earlier, i.e. the critical AC current that needs for system to appear first chaos is smaller.

# Contents

<b>1</b>	<b>Introduction</b>	<b>3</b>
1.1	Josephson effect and Josephson junction . . . . .	3
1.2	RCSJ model: special type of Josephson junction . . . . .	3
1.3	RCSJ Model Analysis and Pendulum Model Fitting . . . . .	4
1.3.1	Situation with resistance (RCSJ Model) . . . . .	4
1.3.2	Pendulum model analogy . . . . .	4
1.4	A brief overview of chaotic systems and terminology . . . . .	4
1.4.1	Chaos . . . . .	4
1.4.2	Bifurcation . . . . .	4
1.4.3	Poincare map . . . . .	5
1.4.4	Running periodic solution . . . . .	5
1.4.5	Kirchhoffs Voltage Law used in previous analysis of RCSJ model circuit . . . . .	5
<b>2</b>	<b>Motivation</b>	<b>5</b>
<b>3</b>	<b>Research Questions</b>	<b>5</b>
<b>4</b>	<b>Literature Review</b>	<b>6</b>
4.1	Pendulum Model analogy: using RCSJ Model . . . . .	6
4.2	Phase portrait of DC current driven Josephson junction and V-I characteristic diagram . . . . .	6
4.2.1	Case 1: Fig. 3(a) . . . . .	7
4.2.2	Case 2: Fig. 3(b) and Fig. 3(c) . . . . .	8
4.2.3	Case 3: Fig. 3(d) and Fig. 3(e) . . . . .	9
4.2.4	Case 4: Fig. 3(f) and Fig. 3(g) . . . . .	9
<b>5</b>	<b>Method</b>	<b>11</b>
<b>6</b>	<b>Results</b>	<b>12</b>
6.1	How changes of $i_a$ influence the system . . . . .	12
6.2	How changes of $\omega$ influence the system . . . . .	15
6.3	How changes of $\beta$ influence the system . . . . .	16
<b>7</b>	<b>Discussion</b>	<b>17</b>
7.1	Summary of our conclusion . . . . .	17
7.2	Why we focus on purely alternating current (why $i_d$ fix 0 all the time?) . . . . .	17
7.3	Why $i_a, \beta$ and $\omega$ influence system in that way . . . . .	18
7.4	Further extension . . . . .	18
7.4.1	Modified Euler method . . . . .	18
7.4.2	Runge-Kutta method . . . . .	18

# 1 Introduction

## 1.1 Josephson effect and Josephson junction

We are familiar with the fact that when a thin insulator is sandwiched between two superconductors, no current can pass through the insulator because it is inherently insulating. However, in 1962, Josephson theoretically predicted a phenomenon that current could pass through this structure without applying any voltage, which named as the Josephson effect<sup>[1]</sup>. He discovered that electrons would form Cooper pairs, so that the two superconducting regions could be described as a single macroscopic wave function that adopts the same phase when the insulator is thin enough, so that there is a voltage difference that allows the current to pass through. The superconductor-insulator-superconductor (SIS) structure in which this Josephson effect occurs is named Josephson junction (Figure 1). Josephson's prediction of zero-voltage currents was later verified by Anderson and Powell in their experiments<sup>[2]</sup>.

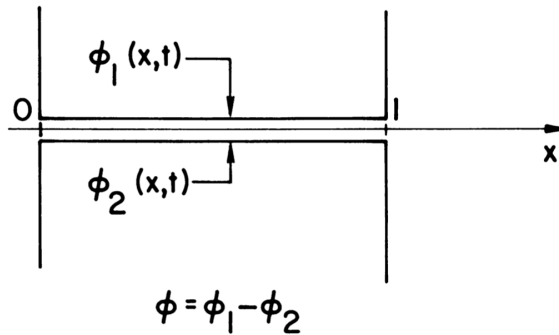


Figure 1: Visualization of a Josephson junction: the model studied here is based on the jump in the electron wave function across the gap, denoted here by  $\phi$ <sup>[3]</sup>

## 1.2 RCSJ model: special type of Josephson junction

There are many types of Josephson junctions, such as  $\pi$ -type Josephson junctions,  $\varphi$ -type Josephson junctions, long Josephson junctions, and superconducting tunneling surfaces and so on, but we now focus on a simpler but extremely versatile model, the RCSJ Model.

RCSJ model referred as the Shunted Linear Resistive Capacitive Junction model. It is a representative one of many Josephson junction models which was proposed by Stewart and McCumber<sup>[5]</sup> in the late 1960's, analogize the junction to circuit demonstrated in Figure 2.

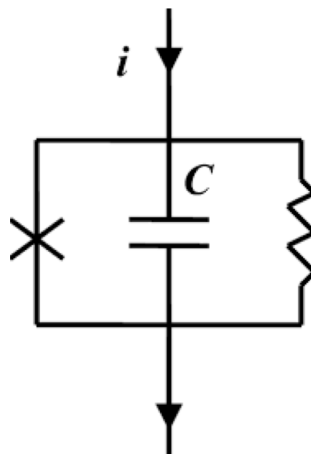


Figure 2: RCSJ model<sup>[5]</sup>

### 1.3 RCSJ Model Analysis and Pendulum Model Fitting

#### 1.3.1 Situation with resistance (RCSJ Model)

When the external current  $I_{ext}$  applied is greater than some critical current  $I_c$ , voltage (V) would be generated over the junction. According to the circuit of RCSJ model, the external current  $I_{ext}$  would be shunted into three sub-stream: one is the through resistance, the other two passing through resistance and capacitance respectively. Applying Kirchhoff's law (see more details in later part 1.4.5) to the circuit, the equation can be developed as:

$$C \frac{dV}{dt} + \frac{V}{R} + I_c \sin \alpha = I_{ext}$$

We also know the Voltage V can also be written as the following expression

$$V = \frac{h}{4\pi e} \frac{d\phi}{dt}$$

(note that  $I_c$ , C, and R are the junction critical current, the junction capacitance, and the junction resistance, respectively,) and the circuit is simulated in Fig.2

Since the junction voltage is given by  $V = \frac{h}{4\pi e} \frac{d\phi}{dt}$ , we plug it in and the equation above can be rewritten as a second-order autonomous system:

$$\frac{hC}{4\pi e} \frac{d^2\varphi}{dt^2} + \frac{h}{4\pi e R} \frac{d\varphi}{dt} + I_c \sin \varphi = I_{ext}$$

where  $h$  is Planck constant,  $\varphi$  is an independent variable.

#### 1.3.2 Pendulum model analogy

The above result is commonly analogized to the pendulum model. We know the pendulum formula is

$$mL^2 \frac{d^2\theta}{dt^2} + b \frac{d\theta}{dt} + mgL \sin \theta = \tau$$

where  $\theta$  is the angle of pendulum. Substitute some variables,  $mL^2 = \frac{hC}{4\pi e}$ ,  $b = \frac{h}{4\pi e R}$ ,  $mgL = I_c$ ,  $I_{ext} = \tau$ . Thus, the pendulum model can be analogized to the RCSJ model.

Also, the complete mechanical analogue of the discrete pendulum model with n coupling junctions for applied torques is given in the literature by Levi and Hoppensteadt in 1976<sup>[3]</sup>, with a detailed analysis of stable static states and solutions with periodic time derivatives. Their results are discussed in detail in the Literature Review section of our paper as well.

### 1.4 A brief overview of chaotic systems and terminology

#### 1.4.1 Chaos

In a chaotic system, the system is very sensitive to the initial value of the motion, despite its determinism. However, the present approximation does not represent the future approximation. Therefore, the unpredictability of the system due to the exponential growth of the error with time is usually considered as a characteristic of chaos.

#### 1.4.2 Bifurcation

Bifurcation theory is a theory that allows for the classification of qualitative changes that occur in a dynamical system. A loss of equilibrium is the simplest type of bifurcation, and it occurs in many physical systems. From a mathematical point of view, the loss of equilibrium is the movement of the zeros of the associated real functions away from the real axis into the complex plane.

### 1.4.3 Poincare map

Poincare mapping is a mapping defined by the motion of orbits in phase space. When the track crosses the same section repeatedly, it reflects the mapping of the dependency between the successor points and the precursor points. The solution of a continuous nonlinear dynamic system is very difficult, so we usually use phase diagram analysis. Although the change of physical quantity with time cannot be quantitatively known in phase diagram, the shape type and topological structure of orbit can be qualitatively obtained, thus the global picture of dynamic system motion can be understood.

### 1.4.4 Running periodic solution

In the current-driven case, a constant current is maintained flowing across the gap, and the resulting voltage is measured. Here, the boundary conditions are

$$\phi_x|x=0 = H \quad \phi_x|x=1 = H + I$$

Where  $I$  is the applied current.  $\phi_t(x, t)$  is typically highly oscillatory, and so time-averages  $\bar{\phi}_t(x, t)$  are actually measured. Such averages exist for solutions whose time-derivatives are periodic. These solutions are so-called running periodic solutions.

By the way, we will see the appearance of the running periodic solutions in our paper. Although in general we meet the periodic solutions as a closed curve, since the system we are studying is in three dimensions, the phase portrait we draw is in the x-y plane. So if we imagine a cylinder, after each cycle, the solution of the differential equation has the same value, so it is indeed a periodic solution.

### 1.4.5 Kirchhoffs Voltage Law used in precious analysis of RCSJ model circuit

Kirchhoffs Voltage Law or KVL, states that “in any closed loop network, the total voltage around the loop is equal to the sum of all the voltage drops within the same loop” which is also equal to zero. This idea by Kirchhoff is known as the Conservation of Energy.

## 2 Motivation

The phenomenon of superconductivity has been a major physical problem that scientists are keen to study, which greatly reduces unnecessary energy consumption, and it is of great importance in the fields of defense, scientific research and industry. Based on the understanding that the Josephson effect is closely related to the concept of superconducting weak coupling, scholars gets rid of the narrow scope of the tunneling phenomenon and expands the type of junction. Josephson junction is the simplest and most fundamental structure in the field of low-temperature superconductivity and it has the advantages of high operating frequency, high speed, high sensitivity, low noise, low power consumption, etc. Scientists have applied the kinetic properties of Josephson junctions in many fields, such as superconducting quantum interference devices (SQUID), hybrids and so on. Josephson junctions with high non-linearity provide an ideal physical system for studying chaos. However, due to its complex dynamical behavior, we are unable to obtain exact analytical solutions in Josephson junctions and related circuit systems, especially for chaotic systems under fully alternating currents and periodic vibrational problems. Therefore, curious about the application of superconductivity and Josephson junction dynamics, we analyzed the behavior of Josephson junction systems and present our results in this paper.

## 3 Research Questions

Based on the above analysis, the main goal of this paper is to focus on system with AC currents with fully alternating currents (implying  $i_d = 0$ ), since they are easier to study and representative enough to account for the evolution of this dynamical system, which will be explained later. For the three remain parameters,  $i_a, \omega, \beta$ , we are going to study how this pendulum analogy system perform with the changes of these parameters.

## 4 Literature Review

### 4.1 Pendulum Model analogy: using RCSJ Model

As mentioned above in our paper, the following differential equation can be obtained from the RCSJ model.

$$C \cdot \frac{dV}{dt} + \frac{V}{R} + I_c \sin \varphi = I \quad (1)$$

According to Dana, Sengupta, and Edoh's analysis<sup>[4]</sup>, if the right hand side of equation (1)  $I$  (the external current) is a constant, then the chaos is ruled out and the system becomes a second order autonomous system. If chaos is needed to be introduced into the system,  $I$  should be changed into a time-periodic force  $I_d + I_a \sin \varphi$  (Notice that if the system is under purely alternating current, then  $i_d = 0$  and if the system is under DC current which means no time-periodic force, then  $I_a \sin \varphi = 0$ ). Thus, the equation can be changed into (2), a second-order non-autonomous system:

$$C \cdot \frac{dV}{dt} + \frac{V}{R} + I_c \sin \varphi = I_d + I_a \sin \varphi \quad (2)$$

and it can be cast into a standard second-order autonomous equation in dimensionless normalized form (four parameters are  $\beta$ ,  $\omega$ ,  $i_a$  and  $i_d$ ):

$$\frac{d^2\varphi}{d\tau^2} + \beta \frac{d\varphi}{d\tau} + \sin \varphi = i_d + i_a \sin(\omega\tau)$$

and we could find the following relations between each paramenters.

$$\begin{aligned} i_a &= \frac{I_a}{I_c} \\ i_d &= \frac{I_d}{I_c} \\ \beta &= \sqrt{\frac{h}{4\pi e I_c C R^2}} \end{aligned}$$

$$\begin{aligned} \tau &= \omega_c t \\ \omega_c &= \sqrt{\frac{4\pi e}{h C}} \\ \omega &= \frac{\omega_a}{\omega_c} \end{aligned}$$

As mentioned before, analogizing to pendulum model,  $\beta$  corresponds to resistance constant and  $i_d + i_a \sin(\omega\tau)$  corresponds to a forcing that supply energy to the system.

### 4.2 Phase portrait of DC current driven Josephson junction and V-I characteristic diagram

In this context, scholars have made a specific study of Josephson junctions ( $i_d \neq 0, i_a = 0$ ) under constant forcing (constant DC current). Such studies greatly simplify the evolution of dynamic systems and exclude chaotic states in the system. For different values of parameters and in combination with the corresponding phase portraits, the V-I characteristic diagram of the DC current junction can be interpreted and understood as well.

In addition to current and voltage, other parameter relationships have been studied, such as Anderson et al. (1963)<sup>[2]</sup> derived junction inductance as a function of temperature and junction current. Therefore, the study of this model is very important to understand the fundamentals of dynamic systems.

We will first study the behavior of different parameters based on other scholars' previous work, focusing in particular on the understanding of Josephson junction under DC current.

The phase diagram of the Josephson junction hand-printed in literature under the driven of DC current is shown in Figure 3 below, and the counterpart can be found in the literature [2]. In order to understand more clearly the characteristics of these phase portraits, we also try to plot the corresponding phase diagram using Mathematica and analyze the periodicity and stability of the solutions for different cases. The figures can be found in each of the following different cases.

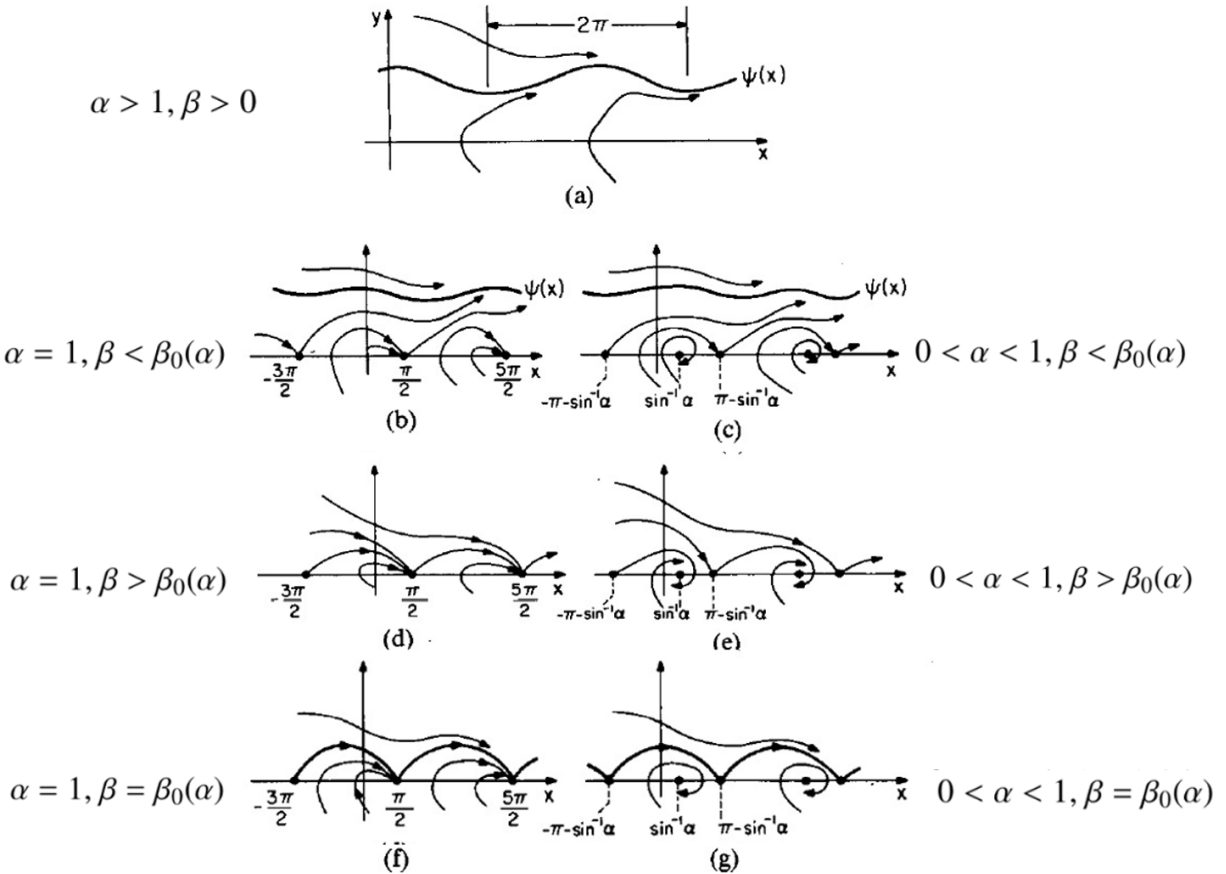


Figure 3: Phase portraits under different conditions ( $\alpha = i_d$  and  $\beta = \sqrt{\frac{h}{4\pi e I_c C R^2}}$ )

According to others analysis, the DC current case is shown to have equilibrium and running periodic solutions, through which the time derivatives of the solutions defined are periodic [5]. Also, in the above mentioned paper [2], the dynamics of Josephson junctions under constant forcing (DC current driven) is studied analytically, with phase diagrams under different conditions.

#### 4.2.1 Case 1: Fig. 3(a)

When  $\alpha > 1, \beta > 0$ , which means  $I_{ext}$  is over some critical current  $I_0$  ( $I_0$  could also be seen in V-I3 characteristic diagram analysis part shown later).

From the phase portrait we plot we can see there exist a unique running periodic solution, which is asymptotically stable. This means each trajectory in the phase plane tends to it as  $t$  goes to  $\infty$ . There are no equilibrium points appear.

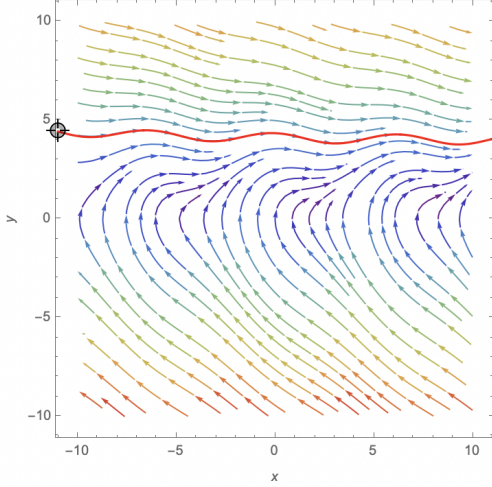


Figure 4: when  $\alpha > 1, \beta > 0$  (x refers to  $\phi$  and y refers to  $\frac{d\phi}{d\tau}$ )

When  $0 < \alpha \leq 1$ , for each  $\beta$ , there should exist a critical value  $\beta = \beta_c(\alpha)$ , which is shown to be a continuous one-to-one function of  $\alpha$ , that divides the dynamics into other three types, which will be discussed in Case 2, Case 3 and Case 4.

#### 4.2.2 Case 2: Fig. 3(b) and Fig. 3(c)

When  $0 < \alpha \leq 1, \beta < \beta_c(\alpha)$ , there exists a unique asymptotically stable running periodic solution and equilibrium points as well. All trajectories outside the attraction of equilibrium tend to the periodic solution. The trajectories inside the attraction of equilibrium tend to the equilibrium points.

Specially, for  $\alpha = 1$ , the equilibrium are located at  $(x, y) = (\pi/2 + 2k\pi, 0), k = 0, \pm 1, \pm 2$ . We can see this result from Fig.3(b).

General case for  $0 < \alpha \leq 1, \beta < \beta_c(\alpha)$ , the equilibrium points located at  $(x, y) = (\arcsin \alpha + 2k\pi, 0)$  are either stable nodes or stable spiral. Those located at  $(x, y) = (\pi - \arcsin \alpha + 2k\pi, 0)$  are saddle points corresponding to Fig.3(c), which is also got from Mathematica shown in Fig.5 below.

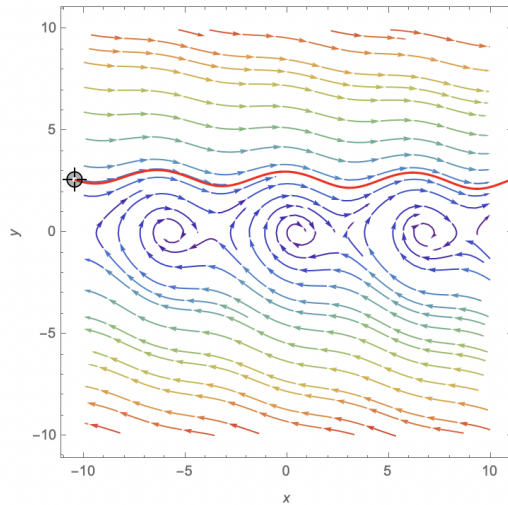


Figure 5: General case for  $0 < \alpha \leq 1, \beta < \beta_c(\alpha)$  (x refers to  $\phi$  and y refers to  $\frac{d\phi}{d\tau}$ )

When  $0 < \alpha \leq 1, \beta \geq \beta_c(\alpha)$ , there are equilibrium but no running periodic solution, which will be discussed in Case 3 and Case 4.

#### 4.2.3 Case 3: Fig. 3(d) and Fig. 3(e)

When  $0 < \alpha \leq 1, \beta \geq \beta_c(\alpha)$ , there are equilibrium but no running periodic solution.

For  $\beta > \beta_c(\alpha)$ , the trajectories tend, either (for  $\alpha = 1$ ) toward the unstable points located at  $(x, y) = (\pi/2 + 2k\pi, 0)$  or (for general case  $0 < \alpha < 1$ ) toward the stable equilibrium at  $(x, y) = (\arcsin \alpha + 2k\pi, 0)$  (except for trajectories converging toward each saddle). This case corresponds to Fig.3 (d) and (e), and (e) is got by Mathematica shown in Fig.6 below.

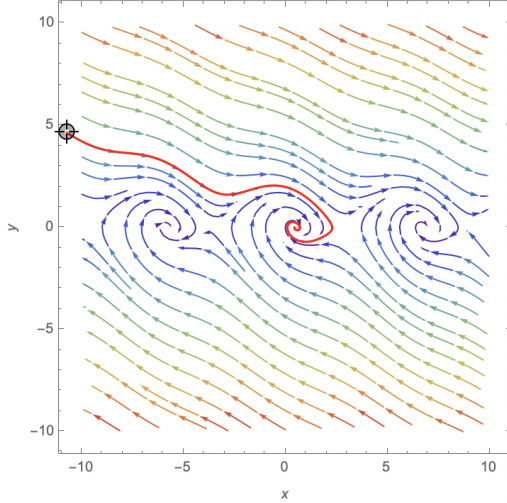


Figure 6: General case for  $0 < \alpha \leq 1, \beta > \beta_c(\alpha)$  ( $x$  refers to  $\phi$  and  $y$  refers to  $\frac{d\phi}{d\tau}$ )

#### 4.2.4 Case 4: Fig. 3(f) and Fig. 3(g)

For  $\beta = \beta_c(\alpha)$ , the trajectories connecting unstable points to form a boundary. Trajectories originating above the boundary tend to it, while trajectories originating below it has the same behavior as in the case 2 ( $\beta > \beta_c(\alpha)$ ). This case corresponds to Fig.4 (f) and (g), and (g) is got by Mathematica shown in Fig.7 below.

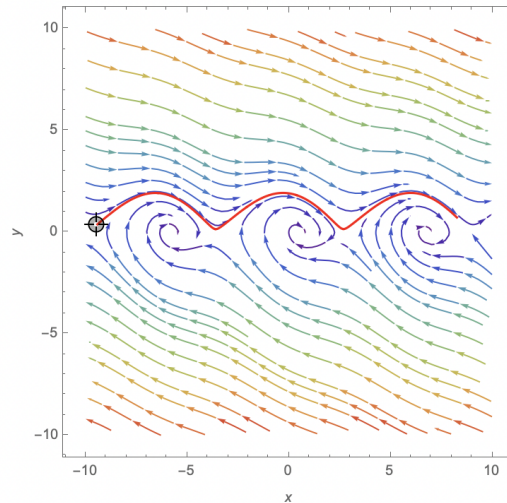


Figure 7: General case for  $0 < \alpha \leq 1, \beta = \beta_c(\alpha)$  ( $x$  refers to  $\phi$  and  $y$  refers to  $\frac{d\phi}{d\tau}$ )

Note: The rigorous proof of the phase portraits for 4 cases can be found in [3].

The V-I characteristic diagram for a fixed  $\beta$  is shown below in Fig.8, which can be explained well using the corresponding phase portraits.

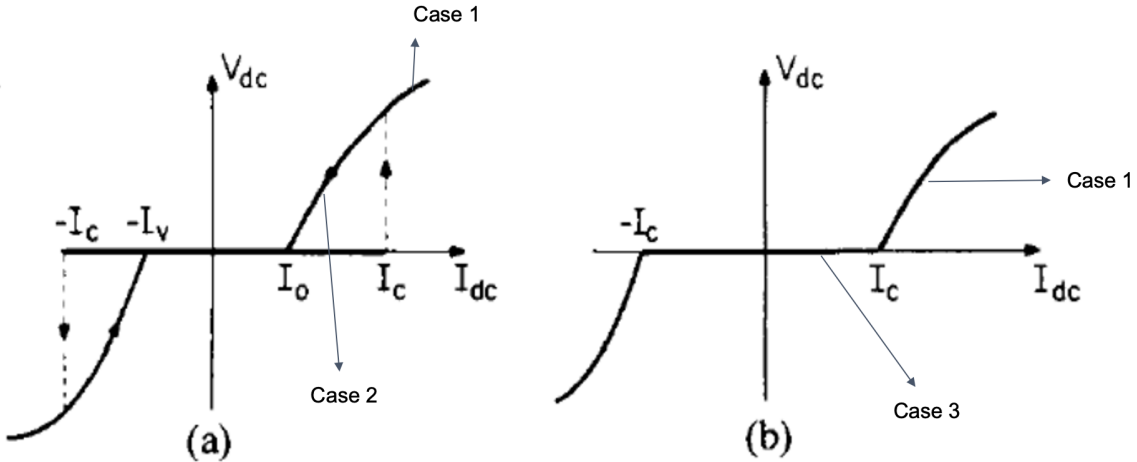


Figure 8: The V-I characteristic diagram for the fixed  $\beta^{[2]}$   
(a) corresponds to  $\beta \leq \beta_c(\alpha)$  and (b) corresponds to  $\beta \geq \beta_c(\alpha)$

This  $I - V$  characteristic diagram corresponds to the physical phenomenon of a DC current driving a Josephson junction, and we can use physical knowledge to understand such a result.

In a Josephson junction device, the voltage response represents the average of the time derivatives of the solution of the equation, so the equation  $y = \frac{d\varphi}{d\tau}$  can be interpreted as the normalized terminal voltage corresponding to the normalized DC input current  $\alpha$ .

When  $\beta > \beta_c(\alpha)$  (Figure 8(b)), for the case where the external current  $I_d$  is smaller than the critical current  $I_c$ , all trajectories in the phase portrait tend to the equilibrium point, in particular, where  $y = 0$  (Case 3, corresponding to Figure 3(e)), so the voltage remains zero, which corresponds to the case where  $I_d$  is smaller than the critical current  $I_c$  in the V-I Diagram (b). For  $\alpha > I_c$ , this corresponds that all trajectories tend to the periodic solution in the phase portraits (Case 1, corresponding to Fig. 3(a)), so the voltage increases with the applied current.

When  $\beta < \beta_c(\alpha)$  (Figure 8(a)), for  $\alpha > I_c$ , the junction behaves approximately the same as  $\beta > \beta_c(\alpha)$  (Case 1, corresponding to Figure 3(a)), we can do similar analysis and the voltage remains zero as well. For  $\alpha < I_c$ , it can be seen from the corresponding phase portrait (Case 2, corresponds to Fig. 3(c)), the trajectory either tends to the periodic solution or tends to equilibrium points. Therefore, the voltage in some areas in the I-V diagram increases with the applied current, and the voltage in some areas always remains 0.

The transition from Figure 8(a) to Figure 8(b) could be achieved by the continued decrease of  $I_d$ . If  $I_d$  continues to decrease,  $\beta_c(\alpha)$  would decrease since  $\alpha$  decreases, so  $\beta$  becomes larger than the original  $\beta_c$  from  $I_0$  to  $I_c$ , which means that now Fig. 8(a) becomes Fig. 8(b). The transition phase from Figure 8(a) to Figure 8(b) corresponds to the case when  $\beta = \beta_c(\alpha)$ , which corresponds to Case 4 (Figure 3(g)).

## 5 Method

We analyzed the behavior of the system as we change parameter values ( $i_a$ ,  $\omega$  and  $\beta$ ) into different regions. The reason why we did not focus on  $i_d$  is that small changes of  $i_d$  would make the system very complex and difficult to observe and analyze, which will be showed in our Discussion part. Here we always keep  $i_d$  at 0 all the time to study the system under purely alternating current.

We first consider the influence of  $i_a$ , which physically means the amplitude of the external alternating current. We decided to draw the Voltage- $i_a$  Bifurcation Diagram with fixed values of  $\beta$  and  $\omega$ , like what are showed in the Literature Review, to see how system perform as  $i_a$  goes through different values. However, the bifurcation diagram is more like an overview, but may hard to be used to study the specific value of  $i_a$  to make the system change its state, thus, phase portraits and Poincare maps are also used in our study, which contributes to know the behavior of the system for a certain  $i_a$ . We used the rough values based on the V- $i_a$  Bifurcation Diagram to draw phase portraits and Poincare maps, and to check whether these values are critical to change the state of system. The reason for lack of calculation process and proof to get these values is that pendulum analogy system with time-periodic driving force is too complicated.

On the top of that, we studied how the system be like with respect with  $\beta$  and  $\omega$ . For  $\omega$ , which is the angular velocity, we decided to draw the V- $i_a$  Bifurcation Diagram with different values of  $\omega$ . For  $\beta$ , which is the damping factor that determines the speed of energy losing for the system, similarly, V- $i_a$  Bifurcation Diagram with different values of  $\beta$  are developed for us to analyze.

## 6 Results

### 6.1 How changes of $i_a$ influence the system

As mentioned in the Method part, we drew the Voltage- $i_a$  bifurcation diagram first to see how the system be like with the respect to  $i_a$  (voltage here refers to  $\frac{d\phi}{d\tau}$ ). To study  $i_a$ , we fixed the values of  $\omega$  and  $\beta$  to 0.5.

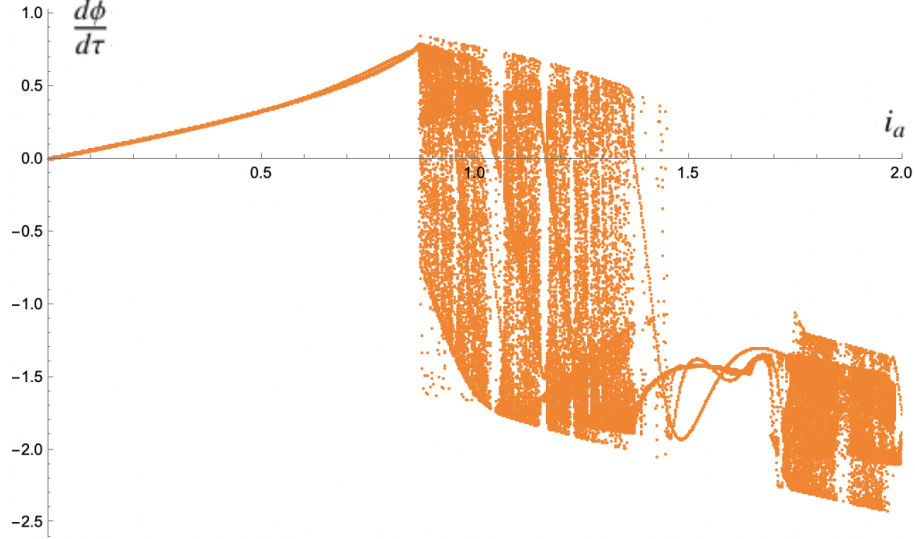


Figure 9: V- $i_a$  Bifurcation Diagram with  $\omega = \beta = 0.5$

It is clear the system perform differently when get different values of  $i_a$ . For the first part of diagram, approximately  $0 < i_a < 0.86$ , the system show the periodicity. Here we chose  $i_a = 0.5$  to draw the corresponding phase portrait and Poincare Map to verify it. The initial point we chose to draw them is the original point.

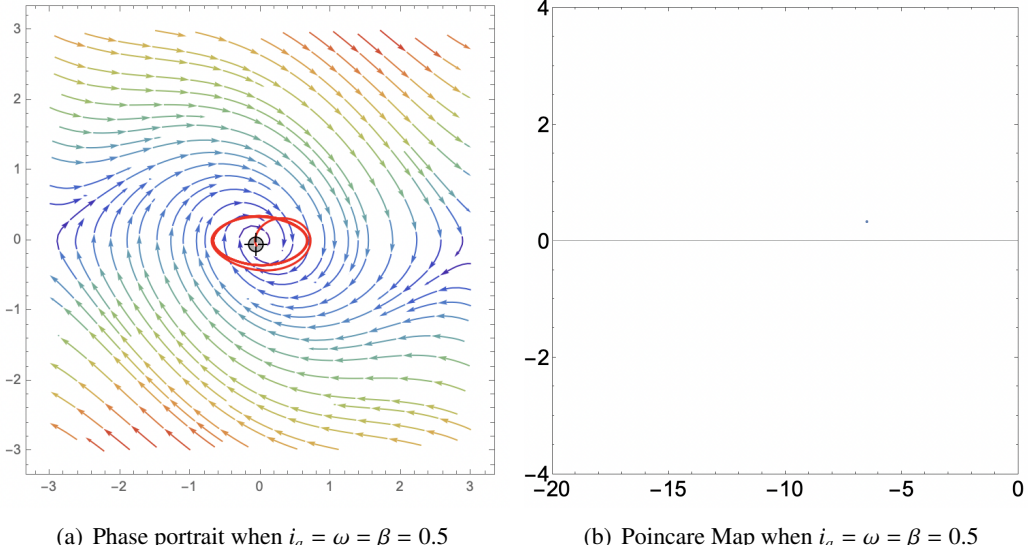


Figure 10: Phase portrait and Poincare Map when  $i_a = 0.5$

Note: The stream-plot in rainbow color is drawn based on the system without the periodic term,  $i_a \sin(\omega\tau)$ , while the red line is draw based on the complete equation. The reason for combining them together is to show the differences between the phase portraits with and without periodic term.

By Fig.10, the red line are approaching the closed trajectory from the original point on phase portrait, while

a single point shown on the Poincare map, which means in this case the period of solution equals to the time interval that we selected for drawing Poincare map, that is  $T = \frac{2\pi}{\omega}$ .

Then, V- $i_a$  bifurcation diagram shows there should be a critical point around  $i_a = 0.86$  to turn the system into chaos from periodicity. To get the value of this  $i_a$ , we drew the phase portraits and Poincare Maps when  $i_a = 0.86$  and  $i_a = 0.87$ .

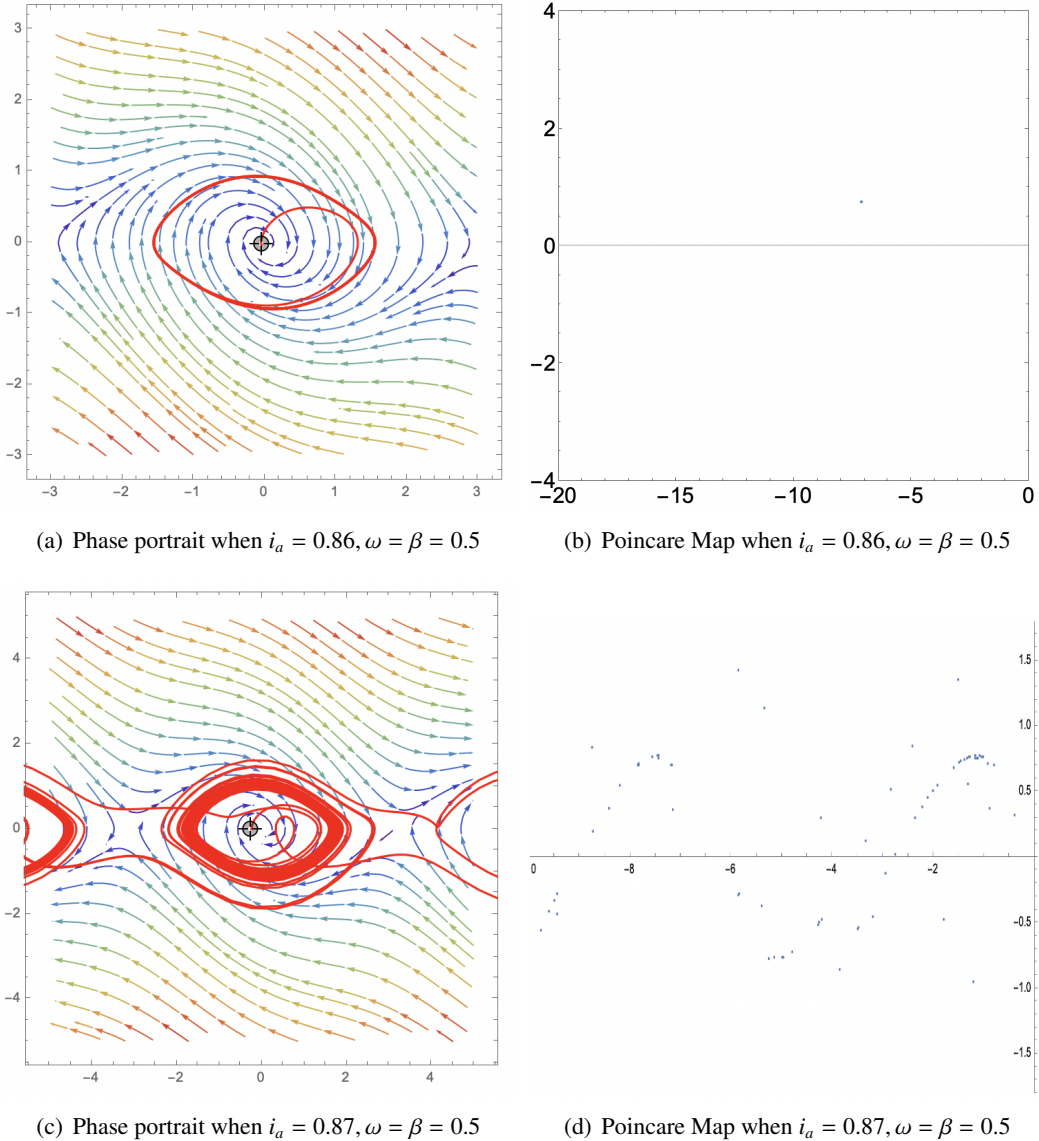


Figure 11: Phase portraits and Poincare Maps when  $i_a = 0.86$  and  $i_a = 0.87$

According to Fig.11(a) and (b), we can observe that the system shows in the similar way as when  $i_a = 0.5$ . The system still has a periodic solution, corresponding to one closed trajectory on the phase portrait and only one point in the Poincare Map. While for  $i_a=0.87$  (Fig.11(c) and (d)), the phase portrait shows that it is no longer a closed trajectory, but relatively chaotic and disordered. The Poincare Map shows many discrete points instead of one point, and these points form a certain shape with periodicity.

V- $i_a$  bifurcation diagram shows that the system becomes a chaotic when  $i_a > 0.87$ . To check it, we used  $i_a = 1.2$  to draw phase portrait and Poincare Map. The results verify that the system is indeed chaos at that time (Fig.12), and more chaotic than when  $i_a = 0.87$ . The phase portrait are more complex and the shape formed by points is more clear that it's periodic on Poincare Map.

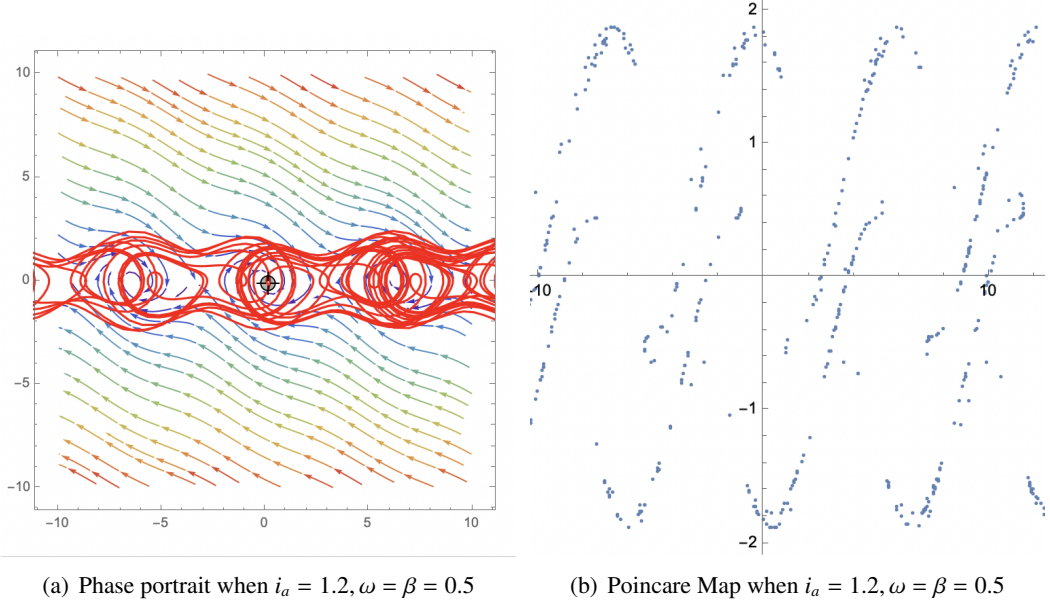


Figure 12: Phase portrait and Poincare Map when  $i_a = 1.2$

When  $i_a$  is around 1.5, the system seems to be less chaotic, which are some lines overlapped instead of completely chaos. The corresponding phase portrait and Poincare Map are shown below.

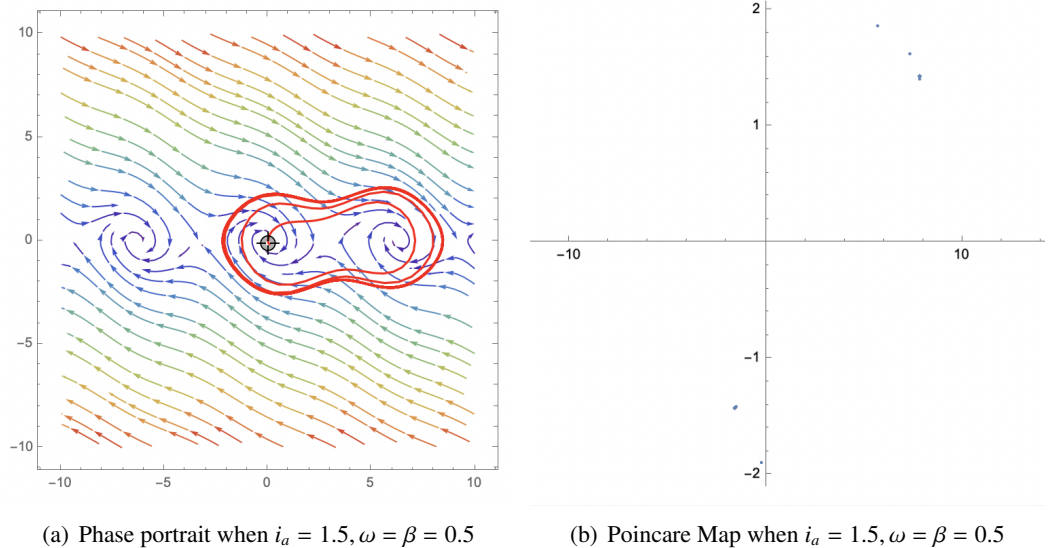


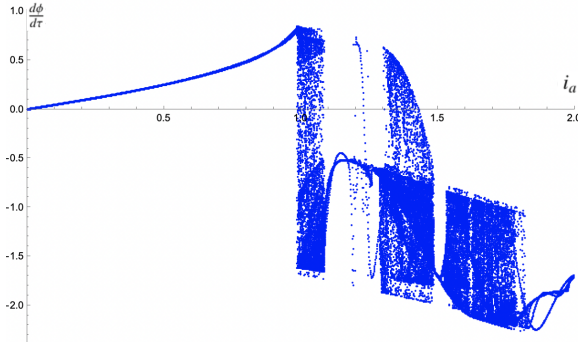
Figure 13: Phase portrait and Poincare Map when  $i_a = 1.5$

By Fig.13, a relatively clear trajectory shown in the phase portrait, but it has the different shape compared to the circumstances when  $i_a < 0.87$ , and points are less and finite in the corresponding Poincare Map. Therefore, for circumstances around  $i_a = 1.5$ , the chaos seems to be weaker and diagram show relative periodicity, although the system will be back to chaos later as  $i_a$  continues to increase. We can get that, after the system turns into chaos for the first time at  $i_a = 0.87$ , as  $i_a$  gets larger, even though it will appear less chaotic or perform periodicity and bifurcation at some certain value of  $i_a$ , the main circumstances are still chaos. However, since relative periodicity and bifurcation may appear from time to time irregularly as  $i_a$  increases, we cannot predict the behavior of this system exactly after first chaos appear.

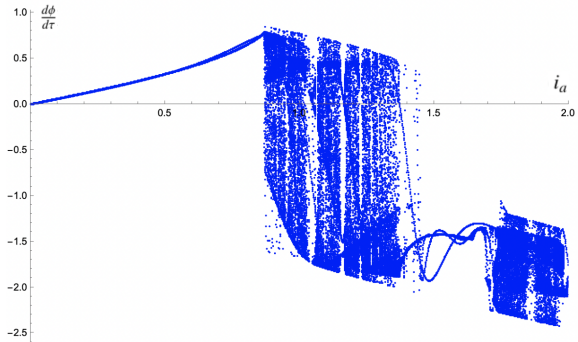
## 6.2 How changes of $\omega$ influence the system

In 6.1, we have already used several phase portraits and Poincare Maps to verify that V- $i_a$  Bifurcation diagram can represent the state of system correctly, so to study  $\omega$  and  $\beta$  in 6.2 and 6.3, we got the results by comparing the V- $i_a$  Bifurcation diagram with the different values of  $\omega$  and  $\beta$ .

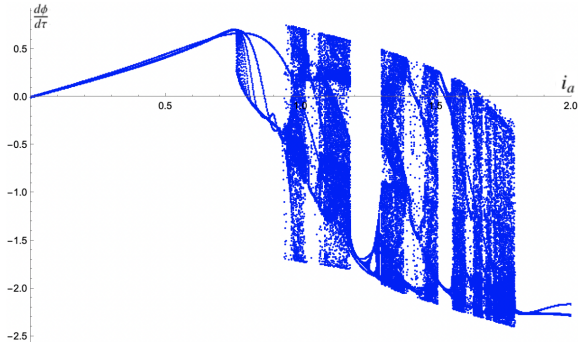
To study  $\omega$ , we fixed  $\beta = 0.5$  as before, but adjust  $\omega = 0.4, 0.5, 0.6$  to see the differences. These three figures are shown below.



(a) V- $i_a$  Bifurcation diagram when  $\omega = 0.4, \beta = 0.5$



(b) V- $i_a$  Bifurcation diagram when  $\omega = 0.5, \beta = 0.5$



(c) V- $i_a$  Bifurcation diagram when  $\omega = 0.6, \beta = 0.5$

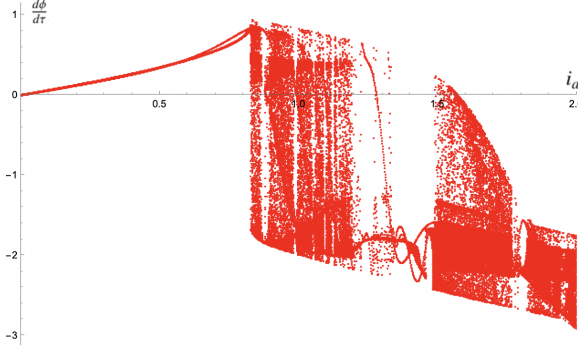
Figure 14: Compare V- $i_a$  Bifurcation diagrams at  $\omega = 0.4, 0.5, 0.6$

Based on Fig.14, changes of  $\omega$  will not influence the general changes of diagram states. For all values of  $\omega$ , the V- $i_a$  Bifurcation diagram show periodicity at the beginning, and will appear chaos later. Then some periodicity and bifurcation will appear from time to time after first chaos appears. As mentioned earlier, the appearance of periodicity and bifurcation are irregular, so it's hard to find pattern after first chaos appears. Therefore, our result about changes of  $\omega$  is only related to the first chaos.

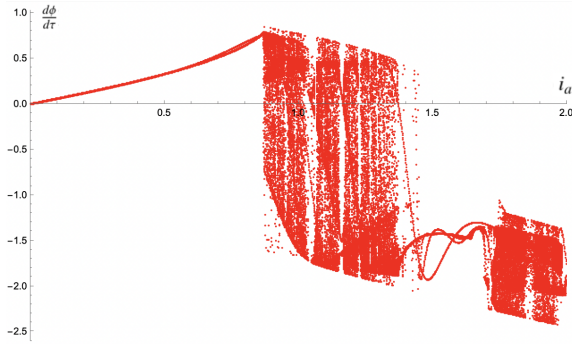
Comparing these three figures, the critical  $i_a$  (the  $i_a$  that makes the system become chaotic for the first time) for  $\omega = 0.4, 0.5, 0.6$  are 0.98, 0.87, 0.76, so it is clear that the appearance of first chaos will be delayed as the  $\omega$  gets smaller.

### 6.3 How changes of $\beta$ influence the system

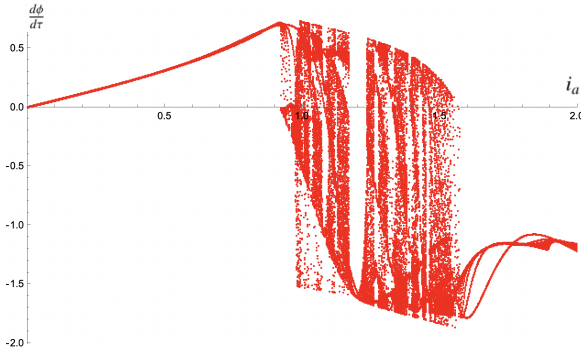
Similarly with 6.2, to study  $\beta$ , we fixed  $\omega = 0.5$  as before, but adjust  $\beta = 0.4, 0.5, 0.6$  to see the differences. These three figures are shown below.



(a) V- $i_a$  Bifurcation diagram when  $\beta = 0.4, \omega = 0.5$



(b) V- $i_a$  Bifurcation diagram when  $\beta = 0.5, \omega = 0.5$



(c) V- $i_a$  Bifurcation diagram when  $\beta = 0.6, \omega = 0.5$

Figure 15: Compare V- $i_a$  Bifurcation diagrams at  $\beta = 0.4, 0.5, 0.6$

Based on Fig.15, changes of  $\beta$  will not influence the general changes of diagram states as well. What's more, the critical  $i_a$  for  $\beta = 0.4, 0.5, 0.6$  are 0.82, 0.87, 0.92, so it is clear that the appearance of first chaos will be delayed as the  $\beta$  gets larger.

## 7 Discussion

### 7.1 Summary of our conclusion

In our paper, we focus on the effect of different values of  $i_a$  on the state of the system, as well as how  $\beta$  and  $\omega$  influence the system. We draw the following conclusions:

1. If the external current is purely alternating ( $I_d = 0$  all the time), for any fixed  $\beta, \omega$ , we can always find a critical current (which we label  $i_{a_c}$ ) such that we can observe chaos for  $i_a > i_{a_c}$  and periodic solutions for  $i_a < i_{a_c}$ . Such a critical current is always existing. For  $i_a < i_{a_c}$ , the system always has periodicity. However, for  $i_a > i_{a_c}$ , the system is not always chaos. Periodicity and bifurcations may appear from time to time and the system will be back to chaos again later.
2. As  $\beta$  increases, we need a large enough  $i_a$  to observe the chaos of the system. This means that as  $\beta$  increases, the moment when the system enters the first chaos is gradually delayed, which means the time to maintain the initial periodic solution will gradually increase, and the moment when the system enters chaos for the first time will be subsequently shifted back. The critical current  $i_{a_c}$  also becomes larger with the increase of  $\beta$ .
3. As  $\omega$  increases, a smaller  $i_a$  allows us to observe the emergence of a chaotic state of the system. As  $\omega$  increases, the moment when the system enters its first chaos will gradually earlier, which means the time to maintain the initial periodic solution will gradually decrease, and the moment when the system enters chaos for the first time will then move forward. The critical current  $i_{a_c}$  also be smaller with the increase of  $\omega$ .

### 7.2 Why we focus on purely alternating current (why $i_d$ fix 0 all the time?)

If we try to plot the bifurcation graph in the case where  $i_d$  is not equal to 0, we may get very complex dynamical systems. The Voltage- $i_a$  Bifurcation Diagram with  $\omega = \beta = 0.5$  and  $i_d = 1$  is shown below.

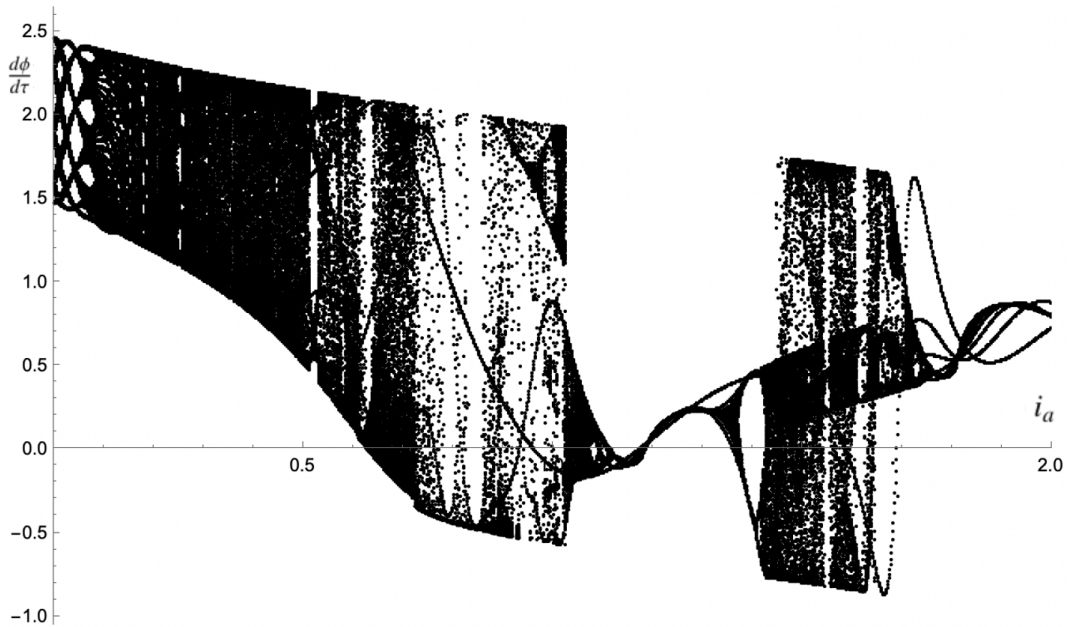


Figure 16: V- $i_a$  Bifurcation Diagram with  $\omega = \beta = 0.5$  and  $i_d = 1$

We can see that it is difficult to determine the state of system and to find the part of periodicity and bifurcation in the chaos. As time goes by, the disorder and unpredictability of the system gradually becomes obvious, which brings a lot of unnecessary trouble to our analysis. That's why we take changes of  $i_a$  out of our study.

### 7.3 Why $i_a, \beta$ and $\omega$ influence system in that way

For the  $i_a$  part, we know that  $i_a$  refers to the magnitude of external force on the system. When  $i_a$  is small, the external force applied to the system is small, so the amplitude of the pendulum is small. Therefore, the single pendulum can keep a single vibration frequency and obey some laws of the linear model. When the magnitude of external force gradually increases, the state of motion becomes a combination of multiple frequencies. If keep increasing, the single pendulum sometimes rotates in the process of vibration. The frequency, position and direction of its vibration and rotation are random and uncertain, which symbolizes the appearance of chaos.

For the  $\beta$  part,  $\beta$  refers to the damping factor, which is attenuation of free vibration caused by various frictional and other hindering effects. For the system to be chaotic, the applied force must first cancel the resistance ( frictional and other hindering effects) before providing the kinetic energy needed for the single pendulum. Thus, the larger the damping factor is, the larger the  $i_a$  (external force) needed for the first chaos, so the critical current  $i_{ac}$  increases as  $\beta$  increases.

For the  $\omega$  part,  $\omega$  refers to angular velocity. With different angular velocities, the period of a single pendulum will be different in relation to the angular velocity. When the angular velocity becomes smaller, the period of the pendulum will become correspondingly larger. When the ideal pendulum is small in  $\omega$ , its motion can be regarded as simple harmonic motion and can be described by simple linear differential equations, but as  $\omega$  increases, its dynamical behavior has to be described by nonlinear equations. Chaos is a random-like behavior in a deterministic nonlinear system that appears to be disorderly but is actually ordered and can occur without any additional random factors. Therefore, first chaos appears earlier with the increase of  $\omega$ .

## 7.4 Further extension

### 7.4.1 Modified Euler method

To make the analysis of the system more accurate, it is proper to use the modified Euler method to solve the equations by approximating the differential to the difference. First use the idea of the forecast-correction method to obtain a prediction in the explicit format, then use the prediction as the initial value of the iteration in the implicit format, and then iterate once to obtain the solution. Once initial conditions are given, the angle and angular velocity of the pendulum at each subsequent moment can be recursively derived, which means as long as we know the angle and angular velocity of the pendulum at the last moment, we can obtain the angle and angular velocity at next moment, and so on repeatedly, the motion of the single pendulum at a series of moments can be predicted.

The overall truncation error of the modified Euler method is related to the time step, so appropriate reduction of the step size helps improve the accuracy of the calculation. However, it will slow down the calculation speed, so we need to weigh the pros and cons of both and choose the appropriate time step for the numerical solution.

### 7.4.2 Runge-Kutta method

As comparison, we can solve the equation using the fourth-order Runge-Kutta method as well. Substituting the specific form of the equation, the specific expression of the computational format is obtained. Similarly, given the initial conditions, the angle and angular velocity of the pendulum at each subsequent moment can be obtained recursively, thus determining the motion of the pendulum. It is known that the overall truncation error of the fourth-order Runge-Kutta method is related to the time step as modified Euler method, but it is a more accurate. The accuracy of fourth-order Runge-Kutta method can be further improved by reducing the time step appropriately.

## References

- [1] B. D. Josephson. The discovery of tunnelling supercurrents. *Reviews of modern physics*, 46(2):251–254, 1974.
- [2] P. W. Anderson and J. M. Rowell. Probable Observation of the Josephson Superconducting Tunneling Effect. , 10(6):230–232, March 1963.
- [3] M. LEVI, F. C. HOPPENSTEADT, and W. L. MIRANKER. Dynamics of the josephson junction. *Quarterly of applied mathematics*, 36(2):167–198, 1978.
- [4] S. K. Dana, D. C. Sengupta, and K. D. Edoh. Chaotic dynamics in josephson junction. *IEEE transactions on circuits and systems. 1, Fundamental theory and applications*, 48(8):990–996, 2001.
- [5] D.E.McCumber. Effect of ac impedance on dc voltage-current characteristics of superconductor weak-link junctions. *Journal of applied physics*, 39(7):3113–3118, 1968.